A note on Pageau et al. (1994) results for the order of stress singularities in multimaterial junctions

Filipe F. Fornazari[a], *Daniane F. Vicentini*[a,b], *Alberto Barroso*[c]

[a]*Group of Advanced Research and Development of Infrastructures*
Department of Transportation, Federal University of Parana
Av. Cel. Francisco H. dos Santos, 210. Jd. das Americas
CEP 81530-000. Curitiba, PR, Brazil.

[b]*Corresponding author: vicentini@ufpr.br*

[c]*Group of Elasticity and Strength of Materials*
School of Engineering, University of Seville
Camino de los Descubrimientos, s/n, E-41092. Seville, Spain.

Abstract

In 1994, Pageau, Joseph and Biggers Jr. evaluated "The order of stress singularities for bonded and disbonded three-material junctions". Their work represented an important finding on multimaterial corners, since their formulation can be used to study the stress state on these junctions. Despite the relevance, the graphs of some results presented in their paper might lead to an improper interpretation, and consequently to a wrong asymptotic stress representation. This is evidenced and discussed in the present work, in which an analytical algorithm was implemented, allowing to reproduce, to complete and to clarify the original results. The physical interpretation of the divergences indicates, among other observations, that the failure mode associated with the highest stress singularity order in a multimaterial junction may change by only varying the Young's modulus of one of the materials.

Keywords: multimaterial junctions, order of stress singularity, Generalized Stress Intensity Factors, Fracture Mechanics

1. Background

Stress singularities are an analytical prediction from the theory of linear elasticity and their study finds applicability in several engineering problems,

as in the analysis of crack propagation through the Stress Intensity Factors (SIFs). Williams (1952) was one of the pioneers in the stress singularities study. Using Airy functions, he investigated angular corners of plates according to the linear elasticity theory. For three boundary conditions (free-free, clamped-free and clamped-clamped), Williams obtained the characteristic equations governing the stresses and displacements in the vicinity of the angular corners. He also extracted the eigenvalues λ for the problem, which would be later called characteristic exponents. These exponents would find direct application in their ability to describe the potential of a given geometry in generating a stress singularity. This potential can be measured by the so-called order of stress singularity δ of the problem, sometimes associated with the very concept of the characteristic exponents λ, commonly defined as $\delta = (1 - \lambda)$ [1] with $0 < \lambda < 1$ (singularity condition).

The work of Williams (1952) included the solution for λ to the classical problem of Fracture Mechanics, i.e., the case of a wedge varying the opening angle between its faces. In a later paper, Williams (1957) used this concept to characterize the stress field in the front of the crack tip (in which $\lambda = 0.5$). In the following decades, several authors devoted efforts to the study of the stress singularity order for different problems, among which are included the multimaterial junctions (also called multimaterial corners).

The evaluation of the eigenvalues λ_k (for k varying from 1 up to n, being n the number of eigenvalues) reached a new level of application when Vasilopoulos (1988) correlated its calculation (from Williams' work, in 1952) with the Stress Intensity Factors (SIFs) from the classical Fracture Mechanics, formalizing the concept of the Generalized Stress Intensity Factors (GSIFs). Thus, as a generalization of the SIFs, the stress field in the vicinity of a point of singularity, under the Linear Elastic Fracture Mechanics (LEFM), could be now generalized by:

$$\sigma_{i,j}(r,\theta) = \sum_{k=1}^{n} \left(\frac{K_k}{r^{1-\lambda_k}} \right) f_{ij}^{k}(\theta) \tag{1}$$

where K_k are the GSIFs, r and θ are the polar coordinates of the point at which the stresses are evaluated and $f_{ij}^{k}(\theta)$ are the characteristic angular functions. The sub index k varies from 1 to n, depending on the problem, generating n terms in the sum (Eq. 1). It is also important to emphasize

[1] See, e.g.,Barroso et al. (2012a)

that Eq. (1) is a stress representation with variable separation, with the role of the radial distance r and the angular position θ being clearly identified. Few exceptional cases do not accept this variable separation, some of those being identified in Sinclair (1999).

The stress field around the crack tip in the SIFs formulation is given by a sum of three terms, each one corresponding physically to a deformation mode. Following this approach, the stress field for other geometries could also be given by a sum of terms, according to Eq. (1), being each mode associated to an eigenvalue λ_k. Related with the studies of the order of stress singularity, the definition of the GSIFs would allow foreseeing a fracture failure criterion for several situations aligned with the practice for crack problems, in which the SIF can be compared to a critical value K_{Ic}, denominated fracture toughness. The GSIFs can be calculated numerically by a method as the one described in Barroso et al. (2012a). For an example of GSIFs being used more recently in a failure criterion, the reader may consult the works of Barroso et al. (2012b) and Vicentini et al. (2012).

For multimaterial corners, studies such as the one of Dempsey and Sinclair (1979) have succeeded in establishing general formulations to obtain the eigenvalues for junctions with an unlimited number of materials converging to one point and several boundary conditions on the faces (or interfaces) between the materials.

Nevertheless, as this kind of analytical general solution may not be practical for some design purposes, particular solutions to simpler problems, such as two or three-material closed corners, are quite useful for engineering problems. Dempsey and Sinclair (1981) have particularized their general solution for bimaterial junctions, directly offering the characteristic equations of the problem under different boundary conditions, making the solution implementation in a straightforward computational code.

For three-material junctions, a particular solution was presented in the paper by Pageau et al. (1994). They used a general solution proposed by Theocaris (1974), who developed a formulation for the problem expressed in complex potentials, in a different way from that in Williams (1952). The authors particularized a solution for four situations: two and three-material corners, considering perfectly bonded interfaces and considering unbonded interfaces. All solutions considered isotropic materials.

This paper concentrates on the formulation for multimaterial closed corners. When implementing a program containing Pageau et al.'s formulation, and trying, first of all, to reproduce their results, some slight differences at

some graphs in the original work led to important physical considerations for the stress representation. Thus, Section 2 briefly reviews the formulation and describes its implementation. Results are presented in Section 3 and discussed in Section 4.

2. Implementation of Pageau et al.'s Formulation

As the solutions employing the method of Williams (1952, 1957), as well as in Dempsey and Sinclair (1979), the solution in complex powers from Theocaris (1974) leads to a system of $4N$ equations (being N the number of materials), which express the stresses and displacements of the problem. For a closed three-material corner with perfectly bonded interfaces, Pageau et al. (1994) presented a system of equations in the form:

$$
\begin{aligned}
\mu_2[\kappa_1 a_{11} e^{2i\lambda\theta_1} - \lambda\overline{a}_{21} e^{2i\theta_1} - \overline{b}_{21}] &= \mu_1[\kappa_2 a_{12} e^{2i\lambda\theta_1} - \lambda\overline{a}_{22} e^{2i\theta_1} - \overline{b}_{22}] \\
[a_{11} e^{2i\lambda\theta_1} + \lambda\overline{a}_{21} e^{2i\theta_1} + \overline{b}_{21}] &= [a_{12} e^{2i\lambda\theta_1} + \lambda\overline{a}_{22} e^{2i\theta_1} + \overline{b}_{22}] \\
\mu_2[\kappa_1 \overline{a}_{21} e^{-2i\lambda\theta_1} - \lambda a_{11} e^{-2i\theta_1} - b_{11}] &= \mu_1[\kappa_2 \overline{a}_{22} e^{-2i\lambda\theta_1} - \lambda a_{12} e^{-2i\theta_1} - b_{12}] \\
[\overline{a}_{21} e^{-2i\lambda\theta_1} + \lambda a_{11} e^{-2i\theta_1} + b_{11}] &= [\overline{a}_{22} e^{-2i\lambda\theta_1} + \lambda a_{12} e^{-2i\theta_1} + b_{12}] \\
\mu_3[\kappa_2 a_{12} e^{2i\lambda\theta_2} - \lambda\overline{a}_{22} e^{2i\theta_2} - \overline{b}_{22}] &= \mu_2[\kappa_3 a_{13} e^{2i\lambda\theta_2} - \lambda\overline{a}_{23} e^{2i\theta_2} - \overline{b}_{23}] \\
[a_{12} e^{2i\lambda\theta_2} + \lambda\overline{a}_{22} e^{2i\theta_2} + \overline{b}_{22}] &= [a_{13} e^{2i\lambda\theta_2} + \lambda\overline{a}_{23} e^{2i\theta_2} + \overline{b}_{23}] \\
\mu_3[\kappa_2 \overline{a}_{22} e^{-2i\lambda\theta_2} - \lambda a_{12} e^{-2i\theta_2} - b_{12}] &= \mu_2[\kappa_3 \overline{a}_{23} e^{-2i\lambda\theta_2} - \lambda a_{13} e^{-2i\theta_2} - b_{13}] \\
[\overline{a}_{22} e^{-2i\lambda\theta_2} + \lambda a_{12} e^{-2i\theta_2} + b_{12}] &= [\overline{a}_{23} e^{-2i\lambda\theta_2} + \lambda a_{13} e^{-2i\theta_2} + b_{13}] \\
\mu_3[\kappa_1 a_{11} - \lambda\overline{a}_{21} - \overline{b}_{21}] &= \mu_1[\kappa_3 a_{13} e^{i\lambda\theta_3} - \lambda\overline{a}_{23} e^{i(2-\lambda)\theta_3} - \overline{b}_{23} e^{-i\lambda\theta_3}] \\
[a_{11} + \lambda\overline{a}_{21} + \overline{b}_{21}] &= [a_{13} e^{i\lambda\theta_3} + \lambda\overline{a}_{23} e^{i(2-\lambda)\theta_3} + \overline{b}_{23} e^{-i\lambda\theta_3}] \\
\mu_3[\kappa_1 \overline{a}_{21} - \lambda a_{11} - b_{11}] &= \mu_1[\kappa_3 \overline{a}_{23} e^{-i\lambda\theta_3} - \lambda a_{13} e^{-i(2-\lambda)\theta_3} - b_{13} e^{i\lambda\theta_3}] \\
[\overline{a}_{21} + \lambda a_{11} + b_{11}] &= [\overline{a}_{23} e^{-i\lambda\theta_3} + \lambda a_{13} e^{-i(2-\lambda)\theta_3} + b_{13} e^{i\lambda\theta_3}]
\end{aligned}
\tag{2}
$$

in which μ_j is the shear modulus of the material j, and κ is the Kolosov constant, given as a function of the Poisson coefficient ν, i.e., $\kappa = (3 - 4\nu)$ for plane strain state, or $\kappa = (3-\nu)/(1+\nu)$ for plane stress state. The angles θ_j define the interfaces between the materials, according to Fig. 1.

For a non-trivial solution to exist (to the unknown constants a_{1j}, $\overline{a}_{2j}$, b_{1j} and $\overline{b}_{2j}$), the determinant of the coefficients matrix must be equal to zero, in

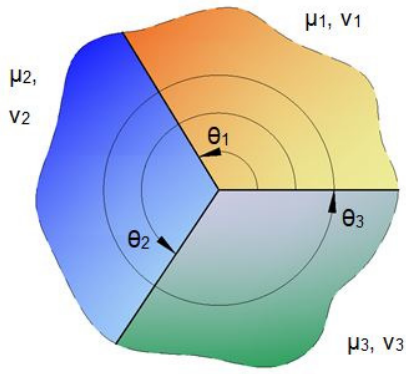

Figure 1: Closed three-material corner.

order to determine λ_k. Thus, the characteristic equation can be implemented in the program and the solution for λ_k can be obtained.

The method of Muller (1956) was chosen to evaluate the eigenvalues of the equation, following Barroso et al. (2003). The solution can be finally obtained by the implementation of the algorithm in a program, here developed in Python 2.7 language (Python Software Foundation). The program's structure and details about its development are presented in Fornazari (2019)'work.

Pageau et al. (1994) used their formulation to plot some graphs, attempted to demonstrate the effect of parameter variation (especially Young's modulus) in the order of stress singularity of the problem (i.e., to study the effect of the stiffness of the materials related on the roots λ_k). They focused on the eigenvalues that would generate singularities, presenting only those with $Re\ \lambda < 1$.

In this paper, the program implemented was used in order to not only reproduce, but also to complete some of those graphs, plotting one additional root (the first non-singular one). During this preliminary stage, some important remarks concerning some particular results of the original paper were observed. These will be detailed in Section 3.

3. Results

In this section, the graphs obtained by Pageau et al. (1994) were re-evaluated and reinterpreted, in comparison to the original ones. These graphs considered the relationship between Young's moduli of two of the materials,

varying the ratio between the moduli of another pair of the corner's materials. In the first case presented here, the authors set $E_1/E_2 = 2.0$, while E_3/E_2 varied. Fig. 2a shows the original graph, while Fig. 2b shows the result obtained by using the algorithm developed in this research. Numbers and other marks in red, over the original graphs, were added for the purposes of this paper. In this example, all roots are real, except for the segment 6 in the original graph (Fig. 2a). The imaginary segment 6 was not depicted in Fig. 2b, in order to allow amplifying the zones of interest. In order to remember that $\lambda_k = 1$ is always a root of this kind of problem, this result was included in all graphs here presented, although in most cases this value is related to rigid rotations—for exceptions, see Vasilopoulos (1988)—and, therefore, this term is not normally considered in the form of Eq. (1).

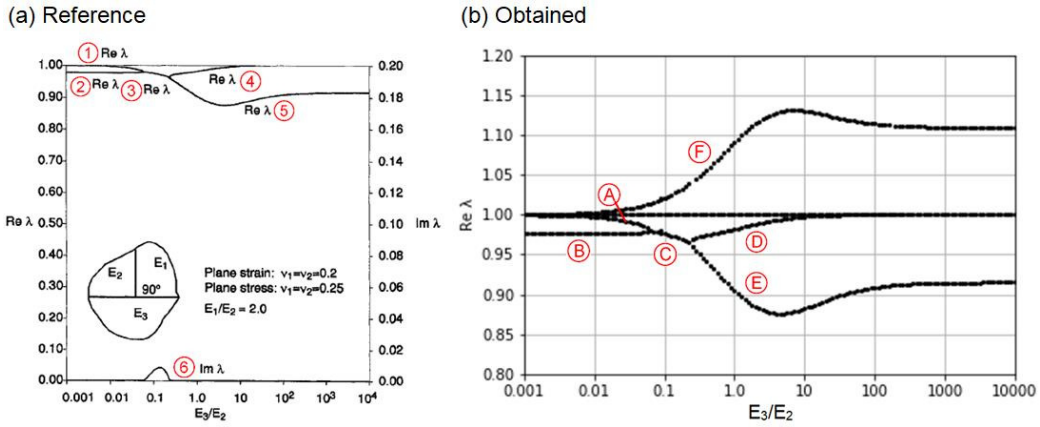

Figure 2: Study of the graph (Fig. 9, in the original source) of Pageau et al. (1994).

One can notice the exact correspondence for the singular results in this case, while, in addition, the curve F in Fig. 2b represents the λ_k associated to the first non-singular term (with values $\lambda_k > 1$).

Note, however, what occurs in the second simulated case, where $E_1/E_2 = 10.0$ is set and E_3/E_2 varies. The roots are all real and the results are shown in Fig. 3.

Since the graph in Fig. 3b (obtained from the algorithm described in Section 2) was generated with a huge number of points, the roots' curves with $Re\ \lambda < 1$ clearly show differences between the connections from the original graph (Fig. 3a). Now it is possible to appreciate that the curves AD and BC in Fig. 3b intersect each other, when compared to their correspondent

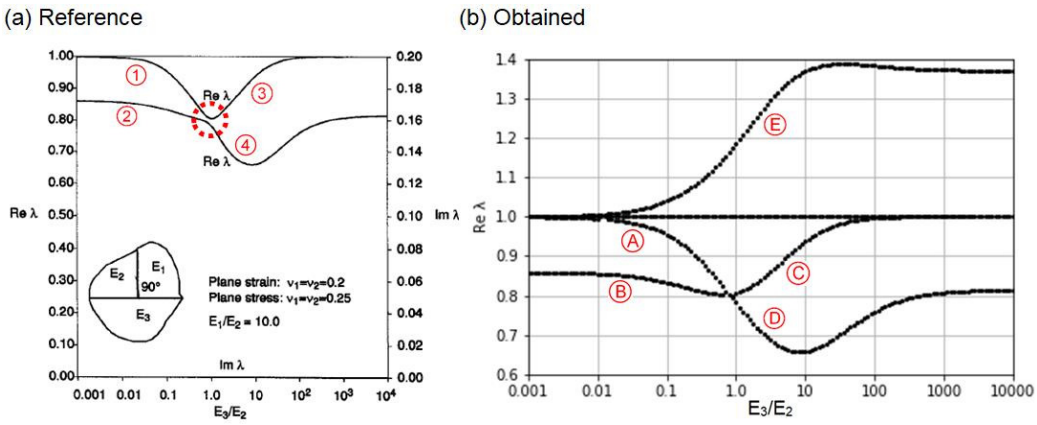

Figure 3: Study of the graph (Fig. 10, in the original source) of Pageau et al. (1994).

in Fig. 3a, where no intersection is visible. This observation can yield to a very important interpretation because, at the intersection point from curves AD and BC (Fig. 3b), singularities change their order of importance in the problem. It is also important the fact that the final representation of stresses (Eq. 1) needs not only the order of stress singularity values but also to properly identify the associated characteristic angular functions. The correct identification of each term in Eq. (1) for each order of stress singularity is of major importance to correctly obtain the asymptotic stress field in the neighborhood of the corner tip. The obtained result clearly shows that the singular terms change their position when crossing $E_3/E_2 \cong 1$, when compared with Pageau et al.'s results. Thus, not identifying this fact, would lead to a wrong stress representation. From this point onwards, i.e., for materials in which Young modulus relationship is $E_3 > E_2$, the previous most singular term becomes less dominant and the reverse occurs when analyzing the other term, which becomes prominent in Eq. (1). Conversely, in the results of Pageau et al. (1994) (Fig. 3a) the singular terms keep their status independently of the materials combination.

In a third problem, Pageau et al. (1994) set $E_3/E_1 = 10.0$ and varied E_2/E_1. The expanded graph, next to the original, is shown in Fig. 4b, where the imaginary parts of the roots (i.e., results with Re $\lambda > 1$) were colored, in order to identify to which real parts they are referring to. Their curves were also identified with the same letters E and H of the real parts, but in a blue tone. By expanding the original graph with a third value of λ_k in Eq. (1), it became clear that the three curves (AC, BG and FD) intersect

themselves at $E_2/E_1 = 1.0$. Thus, in this case, the original results were only complemented.

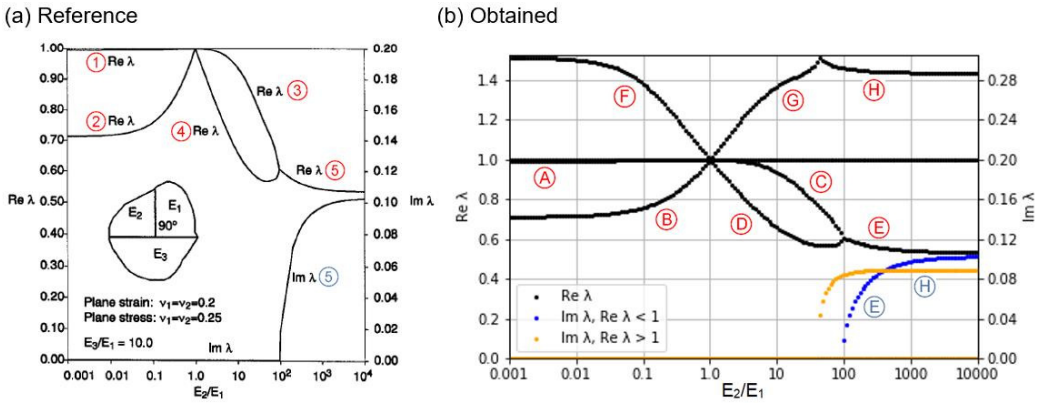

Figure 4: Study of the graph (Fig. 11, in the original source) of Pageau et al. (1994).

Considering that the formulation allows to solve problems of bimaterial corners inclusively (for that, the same parameters are used for materials 2 and 3, and for the angles which define the interfaces), the bimaterial corner graph presented by Pageau et al. (1994) was also re-studied. It is shown in Fig. 5 and, as in Fig. 3, the results show that, unlike the original graph, the segments CF and DE intersect each other for $E_2/E_1 \cong 10.0$. Also, the curves ACF, BH and GDE intersect each other at $E_2/E_1 = 1.0$. The same comments made for results in Fig. 3 can be applied for this case. Although the values of the orders of stress singularities remain almost the same at both sides of the intersection, it is mandatory to correctly relate each term of Eq. (1) to the correspondent value of the order of stress singularity.

4. Discussion

In a practical interpretation from a LEFM point of view, each λ_k is related to a deformation mode of the problem, i.e., a term of the finite sum expressed in Eq. (1). Thus, the λ_k which generally defines the first mode is the smaller one, indicating more potential to generate stress singularities than the other modes.

In the classical crack problem, mode I is called the opening mode and it is associated with normal stresses. Mode II is called the sliding mode and it is associated with in-plane shear stresses. Finally, mode III is called the

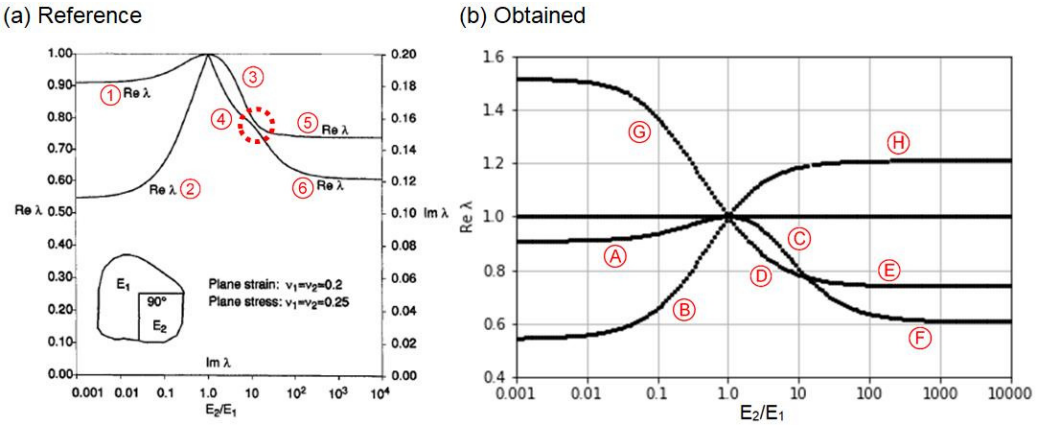

Figure 5: Study of the graph (Fig. 8, in the original source) of Pageau et al. (1994).

tearing mode and it is associated with shear stresses out of the plane of the junction (i.e., torsion). Since that, in this classical problem the eigenvalues are equal (i.e., $\lambda_I = \lambda_{II} = \lambda_{III}$), although generating different eigenvectors, the modes' potential on generating singularity, based on material properties, is the same.

When computing GSIFs for multimaterial corners, the terms in Eq. (1) need to be properly sorted: the first, second and third terms related to Mode 1, 2 and 3 of deformation, respectively (most terms, if they exist, are generally neglected in the vicinity of the corner tip). This also implies that, if the corner is in pure mode 2, the singularity order of the problem must be given as a function of λ_2, even though the λ_1 of the geometry is smaller (i.e., $\lambda_1 = 0$ in this example).

Considering this assumption, the results in the first case (Fig. 2b) show that the eigenvalues of mode 3 (curve F) do not generate a stress singularity ($\lambda_3 > 1$), so that the order of singularity of this corner is, for any E_3/E_2, higher in the first two modes, which tends to be dominant in the stress field.

Nevertheless, in the second case (Fig. 3b), two curves (AD and BC) intersect each other, differently from the original graph (Fig. 3a), where curves apparently do not touch each other. This means that curve AD corresponds to λ_2 domination before the crossing point and λ_1 domination beyond that point. So, if the physical meaning of the modes is being considered, the smallest λ_k of the problem, for a case with $E_3/E_2 < 1.0$, should not be automatically assigned to mode 1.

This is even clearer in the third case. Even though the results for non-singular terms in Fig. 4b are not presented in Fig. 4a, the mode that begins with the greater order of singularity on this corner loses the capacity to even generate a stress singularity for values of $E_2/E_1 = 1.0$ (curve BG, in the graph, Fig. 4b). Likewise, the weaker mode for $E_2/E_1 < 1.0$ (curve FD, in the graph) becomes dominant after the crossing point. By imagining an engineering problem in which one intends to design a three-material junction submitted to a specific stress state (with two materials already defined), these results would indicate that the choice of the third material may imply whether or not a stress singularity in the corner will occur.

Finally, the results for the bimaterial corner (Fig. 5b) show two intersections (for $E_2/E_1 = 1.0$ and for $E_2/E_1 \cong 10.0$). Thus, in this case, the initially λ_2 (from curve ACF) changes significantly the dominance along the proper E_2/E_1 combination.

5. Conclusion

Engineering problems have, historically, found significant applicability to the study of stress singularities, despite these are only theoretical predictions from linear elasticity. If the SIFs, for the study of crack propagation, are the most widespread parameter on this topic, the GSIFs can also be quite useful in defining failure criteria for various problems.

The order of stress singularity of a multi-material corner indicates the potential that the geometry has in generating a singularity, with greater or lesser intensity. Several studies have been conducted over the years to calculate this parameter.

In the present work, the formulation of Pageau et al. (1994) was chosen to evaluate the orders of stress singularity for the multimaterial corners. Some results were re-evaluated by expanding the original graphs of Pageau et al. (1994). In the re-evaluation of these plots, it was found that two of the original graphs might lead to an improper definition of the singular terms in the stress field representation, since the curves of the eigenvalues λ_k should actually intersect each other, a result which is not visible in the original cited paper.

The intersection of the curves means that the failure mode guided by the highest order of singularity in a corner may vary for different material combinations. By analogy with the classical LEFM, the opening mode may have greater potential to produce singularity in a given junction, while the sliding

mode may have a greater order of singularity in another similar junction, in which only one of the materials is modified. And it is even possible that the most important failure mode in a material combination does not even generate a stress singularity in another material combination, to the same geometry.

Acknowledgements

The authors would like to thank the National Department of Transportation Infrastructure of Brazil (DNIT) for the support granted to the first author of this paper. This work was carried out in the Postgraduate Program in Civil Construction Engineering of the Federal University of Parana, Brazil.

References

A. Barroso, V. Mantič, and F. París. Singularity analysis of anisotropic multimaterial corners. *International Journal of Fracture*, 119(1):1–23, 2003. doi: 10.1023/A:1023937819943.

A. Barroso, E. Graciani, V. Mantič, and F. París. A least squares procedure for the evaluation of multiple generalized stress intensity factors at 2d multimaterial corners by bem. *Engineering Analysis with Boundary Elements*, 36(3):458–470, 2012a. doi: 10.1016/j.enganabound.2011.09.011.

A. Barroso, D. Vicentini, V. Mantič, and F. París. Determination of generalized fracture toughness in composite multimaterial closed corners with two singular terms–part i: Test proposal and numerical analysis. *Engineering Fracture Mechanics*, 89:1–14, 2012b. doi: 10.1016/j.engfracmech.2011.12.014.

J.P. Dempsey and G.B. Sinclair. On the stress singularities in the plane elasticity of the composite wedge. *Journal of Elasticity*, 9(4):373–391, 1979. doi: 10.1007/BF00044615.

J.P. Dempsey and G.B. Sinclair. On the singular behavior at the vertex of a bi-material wedge. *Journal of Elasticity*, 11(3):317–327, 1981. doi: 10.1007/BF00041942.

F.F. Fornazari. Análise dos fatores de intensidade de tensão generalizados em quinas multimateriais existentes na junção entre pavimentos flexíveis e pontes. Master's thesis, Federal University of Parana, Brazil, 2019.

D.E. Muller. A method for solving algebraic equations using an automatic computer. *Mathematical tables and other aids to computation*, 10(56):208–215, 1956. doi: 10.2307/2001916.

S.S. Pageau, P.F. Joseph, and S.B. Biggers Jr. The order of stress singularities for bonded and disbonded three-material junctions. *International Journal of Solids and Structures*, 31(21):2979–2997, 1994. doi: 10.1016/S0020-7683(97)00108-X.

Python Software Foundation. Python language reference, version 2.7.14. `https://www.python.org/`. Last accessed: 2019-07-27.

G.B. Sinclair. Logarithmic stress singularities resulting from various boundary conditions in angular corners of plates in extension. *Journal of applied mechanics*, 66(2):556–559, 1999. doi: 10.1115/1.2791085.

P.S. Theocaris. The order of singularity at a multi-wedge corner of a composite plate. *International Journal of Engineering Science*, 12(2):107–120, 1974. doi: 10.1016/0020-7225(74)90011-1.

D. Vasilopoulos. On the determination of higher order terms of singular elastic stress fields near corners. *Numerische Mathematik*, 53(1-2):51–95, 1988. doi: 10.1007/BF01395878.

D. Vicentini, A. Barroso, J. Justo, V. Mantič, and F. París. Determination of generalized fracture toughness in composite multimaterial closed corners with two singular terms–part ii: Experimental results. *Engineering Fracture Mechanics*, 89:15–23, 2012. doi: 10.1016/j.engfracmech.2012.02.017.

M.L. Williams. Stress singularities resulting from various boundary conditions in angular corners of plates in extension. *Journal of applied mechanics*, 19(4):526–528, 1952.

M.L. Williams. On the stress distribution at the base of a stationary crack. *Journal of applied mechanics*, 24:109–114, 1957.